Characterization of bottom sediment resuspension events observed in a micro-tidal bay

Manel Grifoll[1,2], Pablo Cerralbo[1,2], Jorge Guillén[3], Manuel Espino[1,2], Lars Boye Hansen[4], Agustín Sánchez-Arcilla[1,2]

[1]Laboratori d'Enginyeria Marítima, Universitat Politècnica de Catalunya (UPC-BarcelonaTech), Barcelona, 08034, Spain
[2]Centre Internacional d'Investigació dels Recursos Costaners (CIIRC), Barcelona, 08034, Spain.
[3]Institut de Ciències del Mar (ICM-CSIC), Barcelona, 08003, Spain.
[4]DHI-Gras, Horsholm, DK-2970, Denmark.

Correspondence to: Manel Grifoll (manel.grifoll@upc.edu)

Abstract. In this contribution we investigate the origin of the variability in near-bottom turbidity observations in the Alfacs Bay (NW Mediterranean Sea). This bay is characterized by a micro-tidal environment and a relevant seiching activity which may lead to flow velocities of more than 50 cm•s-1. A set of current meters and optical sensors mounted near the sea bottom were used to acquire synchronous hydrodynamic and optical information of the water column. The time-series observations showed an evident relation between seiche activity and sediment resuspension events. The observations of turbidity peaks are consistent with the node/anti-node location for the fundamental and first resonance periods of the bay. The implementation of a coupled wave-current numerical model shows a strong spatial variability of the potential resuspension locations. Strong wind events are also a mechanism responsible of the resuspension of fine sediment within the bay. This is confirmed using retrieval of suspended sediment concentration from Sentinel-2 data. We suggest that the sequence of resuspension events plays a relevant role in Suspended Sediment Concentration, in such a way that previous sediment resuspension events may influence the increase of suspended sediment in subsequents events. The suspended sediment events likely affect the ecological status of the bay and the sedimentary process at long-term period.

1 Introduction

Suspended sediment in the water column and subsequent deposition plays a critical role in coastal environment and management. High levels of suspended sediment concentration in the water column has relevant implications in aquatic ecosystem and natural habitat (Ellis et al., 2002) in particular during large exposure periods ((Newcombe and Macdonald, 1991). Also, sediment supplied from rivers transports load of organic matter, pollutants and heavy metal that may be deposited in the vicinity sea bottom or transported offshore (Palanques et al., 2017). The sediment dynamics is relevant in coastal bays and estuaries due to the large amount of sediment delivered by the freshwater and the potential fine sediment trapping zones. In addition, sediment resuspension can results in a large contribution to the total nutrient load (Sondergaard et al., 1992) and

prevent the sunlight penetration (Mehta, 1989). Besides, the analysis and prevention of fine sedimentation within basins and channel access is object of investigation in port engineering context in order to examine the siltation process (e.g. (Ghosh et al., 2001; van Maren et al., 2015)). Finally, the growth of harmful species, such as dinoflagellate cysts, may be related to significant local resuspension through the mixing of the upper layers, resulting to more homogenous cyst profiles in the sediment (Giannakourou et al., 2005).

In coastal area, the transport sediment is related with the hydrodynamic conditions. In large time scales advection processes redistribute and determine the final depositional pattern as a function of the sediment and water current variables (Bever et al., 2009; Ogston et al., 2000). Hydrodynamics processes driven by wind-waves (Carlin et al., 2016; Grifoll et al., 2013), tides (Fan et al., 2004; Garel et al., 2009), winds (Hofmann et al., 2011; Sherwood et al., 1994), surface seiches (Jordi et al., 2008) or internal-seiches (Shteinman et al., 1997) promote the resuspension, advection and settling of fine sediment conditioned by the continental sediment sources. Subsequent resuspension effects due to natural causes also contributes at the reworking and final deposition of the sediment load (Grifoll et al., 2014a; Guillén et al., 2006). In this sense, anthropogenic activities such as, fishing trawling, ship propellers and waves generated by vessels may bring additional energy in the water system influencing the resuspension, transport and final sediment deposition in shallow waters (e.g. (Garel et al., 2009; Hofmann et al., 2011).

Alfacs Bay (NW Mediterranean Sea; Southern part of the Ebro Delta) is a micro-tidal estuary and intensively exploited area with tourism, fishing and aquaculture activities being an ecosystem of relevant economic importance in the region. It has been investigated extensively in the past in terms of hydrodynamics response (Cerralbo et al., 2015a, 2016, 2018; Llebot et al., 2014; Solé et al., 2009), tidal wave propagation (Cerralbo et al., 2014), biochemical processes (Llebot et al., 2010, 2011) an optical water properties (Ramírez-Pérez et al., 2017). The estuary receives freshwater discharge from the rice fields of the Ebro river. Thus, Alfacs Bay is an intensively exploited area with tourism, fishing and aquaculture activities being an ecosystem of relevant economic importance in the region. Several episodes of algal blooms (linked with the increase of nutrients and perhaps triggered by resuspension mechanisms) and presence of harmful bacterium in bivalve with negative effects on aquaculture have been reported (Loureiro et al., 2009; Roque et al., 2009).

With the purpose to improve the knowledge in fine sediment dynamics in coastal bays, the goal of this investigation is to provide a physical interpretation of the sediment resuspension events observed within a micro-tidal bay (Alfacs Bay; NW Mediterranean Sea). Using sea-level, water currents and wind measurements we investigate the driving mechanisms that resuspend fine bottom sediment within the bay. Then, the spatial and temporal interpretation of the resuspension mechanisms linked with the hydrodynamics is analyzed through the implementation of a wave-current coupled numerical model. The contribution aims to provide explanation of resuspension mechanisms; the knowledge of these mechanism may have an evident benefit for human activities management mentioned previously (e.g. harmful species resuspension or algal blooms with negative effects on aquaculture activities).

The water circulation in Alfacs Bay has been widely analyzed in previous contributions using observational data set and numerical results (Camp and Delgado, 1987; Cerralbo et al., 2014, 2015a; Llebot et al., 2014). However, fine sediment dynamics and its resuspension mechanisms has not been examined yet. Synchronous optical measurements, jointly with velocity and sea-level measurements, have entailed a good chance to investigate the resuspension mechanisms in Alfacs Bay. This area is an example of micro-tidal estuary, thus being the wind or wind-waves candidates mechanisms of fine sediment dispersal.

2 Methods

2.1 Study Area

Alfacs Bay, located at south of the Ebro delta, is formed by the prograding southern spit. The semi-enclosed bay is about 16 km long and 4 km width. The average depth is 4 m and the maximum depth is about 6.5 in the middle of the bay (Figure 1). The connection with the open sea is 2.5 km, with a central channel of 6.5m and shallow edges of around 1-2 m on both sides. The bay is surrounded by rice fields to the north, which spill around 10 $m^3 \cdot s^{-1}$ of freshwater loaded with nutrients during 9-10 months per year (April-December) distributed in several channels, and a sand beach closing it on the east side. The seabed in the central part of the bay is composed by very fine sediment (typically 65-65% silt, 30-35% clay and around 5% sand) increasing the sandy content towards the edges of the bay (Guillén and Palanques, 1997; Satta et al., 2013). The bottom sediment of Alfacs is composed of mud, with significant content of clay, and sand (Palacín et al., 1991). They found that the muddy sediment extended by the central part of the bay and the content of sand increased near to spit that separate the bay from open sea and also in the southern shallow edge.

The bay has been defined as a salt-wedge estuary (Camp and Delgado, 1987) with almost stable stratification all year. The highest tidal range during spring tides is around 0.2 m, and the hydrodynamic fluctuations are controlled by the wind modulated by the seiche activity in a short periods (Cerralbo et al., 2015a). The water circulation in the low-frequency band is dominated by both winds and salinity gradients due to freshwater discharge (Solé et al., 2009; Cerralbo et al., 2018). The most intense regional winds in the area are from the north and northwest, establishing a wind jet due to the orographic effects in the Ebro River valley (Grifoll et al., 2015, 2016). This offshore wind is characterized by noticeable spatial variability due to the surrounding topography (Cerralbo et al., 2015b). The water column within the bay used to be stratified due to the freshwater discharge, but well-mixed conditions are common during winter as a consequence of the hydrodynamic response to strong wind forcing (Llebot et al., 2014) and occasionally to seiches (Cerralbo et al., 2015a). During summer, the contribution of the temperature at the stratification may be also substantial (Cerralbo et al., 2015a).

2.2 Measurements campaigns

The bulk of the observational data correspond at two months field campaign from July to mid-September 2013. The data set consisted of water currents from two 2MHz Acoustic Doppler Current meter Profiler (ADCPs) moored in the mouth (A1) and inner bay (A2) (Fig.1) configured to record 10 min averaged data from 10 registers per minute and with 25 cm vertical cells. Both devices were equipped with Optical Backscatter Sensor (Campbell Scientific OBS-3), bottom pressure meter and a temperature sensor, and they were mounted on the sea bottom at 6.5 m depth. OBS signal is transformed to Nephelometric Turbidity Units (NTU) using device calibration. Besides, the study area used to present a linear relation between optical signal and suspended sediment concentration (Guillén et al., 2000). The distance of the ADCPs and OBS sensor were 0.25 m above the sea bed. The ADCP has a 20 cm of blanking zone. Additional sea level data were obtained through a sea level gauge mounted in Sant Carles de la Ràpita harbor (Fig.1) and bottom pressure systems from the ADCPs. Atmospheric data (wind, atmospheric pressure, solar radiation and humidity) were obtained from a land station located in Sant Carles de la Ràpita (M-Sc) mounted 10 m above the ground.

2.3 Current and wave model implementation

We use the coupled version of SWAN-ROMS models included in the COAWST system in order to simulate the hydrodynamics within the bay. The COAWST system (Warner et al., 2010) consists of several state-of-the-art numerical models that include ROMS (Regional Ocean Modeling System) for ocean and coastal circulation and SWAN (Simulating Waves Nearshore) for surface wind-wave simulation. SWAN is a third-generation numerical wave model that computes random, short-crested waves in coastal regions with shallow water and ambient currents (Booij et al., 1999). It is based on the wave action balance with sources and sinks and incorporates the state-of-the-art formulations of the processes of wave generation, dissipation and wave-wave interactions. ROMS is a three-dimensional circulation model which solves the primitive variables on a sigma-level in the vertical and horizontal regular grid. Numerical aspects of ROMS are described in detail in (Shchepetkin and McWilliams, 2005). In COAWST system, the wave model provides hydrodynamic parameters (i.e., significant wave height, average wave periods, wave propagation direction, near-bottom orbital velocity and wave energy dissipation rate) to the water circulation model. The ocean model provides water depth, sea surface elevation, and current velocity to the wave model. The variables exchange is made “on-line” during the simulation processes, via Model Coupling Toolkit (Jacob et al., 2005), where a multi-processes MPI protocol is used to distribute the computations among several nodes. The COAWST also include different formulations to parametrize the wave-current bottom boundary layer and the wave effect on currents (Warner et al., 2008; Kumar et al., 2012).

The implementation of the COAWST system in Alfacs Bay consisted of a regular grid of 186 x 101 points with a spatial resolution of 100 m (in both x and y) and 12 sigma levels in the vertical. Details of the implementation and the skill assessment of the ROMS model in Alfacs Bay is provided in (Cerralbo et al., 2015a). The same regular grid is used by the SWAN model.

A two-year water circulation simulation (2012-2013) was performed in order to obtain realistic three-dimensional temperature and salinity fields. The barotropic time step was 30 s for ROMS and SWAN solved the wave field each 3600 s. The interval time between change of variables of ROMS and SWAN was established in 3600 s. For both simulations, open boundary was forced with depth-averaged velocities and sea level measured at A1 (interval data of 600 sec). The freshwater inputs are distributed on 8 points simulating the main rice channels with a total flow of $10 m^3 s^{-1}$ (see (Cerralbo et al., 2015a)).

The bottom boundary layer was parameterized using the combined wave-current (Styles and Glenn, 2000) adopted in ROMS and SWAN coupling in (Warner et al., 2008). The input parameters for the model are the velocity components near the bottom and wave characteristics near the bottom (wave period, wave direction and the wave orbital direction). For each computational step, an initial assessment of bed roughness length is estimated as a function of the grain size, ripples and sediment transport. Then, the pure current (τ_c) and pure wave (τ_w) bottom stress are computed as:

$$\tau_c = \frac{(u^2+v^2)\kappa^2}{\ln^2(z/z_0)} \quad (1)$$

$$\tau_w = 0.5 f_w u_b^2 \quad (2)$$

where z is the vertical coordinate, u and v are the water speed, u_b is the orbital velocity, κ is the von Karman's constant, and f_w is the Madsen wave-friction factor. Then, the maximum bottom stress under wave-current conditions is computed as (Soulsby, 1997):

$$\tau_{wc} = \tau_b \left(1 + 1.2 \left(\frac{\tau_w}{\tau_w+\tau_c}\right)^{1.5}\right) \quad (3)$$

The wave effects on currents are considered using vortex-force formalism, which is included in COAWST. This approach allows to consider the effect of the gravity waves on the mean flow and was tested in different experimental and real configurations by (Kumar et al., 2012).

3 Results

3.1 Observations

In order to investigate the suspended sediments events within Alfacs Bay we use a sub-set of the total observations recorded in A2: from 2nd August to 8th August 2013. This is because the sub-set data selected include the main hydrodynamic conditions susceptible to increase the near-bottom turbidity. Figure 2 show the time-series recorded in A2 in terms of NTU from the OBS, sea level height measured (additionally sea-level height measured in A1 is also shown), bottom current speed in m•s-1 in A1

and wind speed and direction measured in M-Sc (see Figure 1). The sea level height reference was obtained subtracting the mean value of the pressure meter time-series provided by the ADCP.

The wind characterization (Figure 2.a and 2.b) include two of the most typical situations in the region: sea breeze and the NW winds (Cerralbo et al., 2015a). The sea breeze is associated to an increase of wind speed during the central hours of the day (approximately from 11:00 hr to 18:00 hr with a wind direction within the range 30º to 180º approximately). From a daily point of view, this seems evident during the 1st to 6th of August. A different pattern is observed during the wind speed peak of 7th-8th of August where 330º wind direction were measured. This corresponds to an offshore wind typical from the region (NW winds called "Mestral").

The period of analysis, also include a seiche event during the 3rd of August. This seiche event was previously characterized hydro-dynamically in Cerralbo et al., (2015a) revealing a characteristic oscillation of 1 hour period in sea-level and currents. This oscillation is characterized by a node (approximately located at A2) where the velocities are maximum, and an anti-node (approximately located in A1) where the amplitude is maximum (see sea-level height in A1 in comparison to A2 in Figure 2.c). The homogeneous vertical profile in velocities measured in A2 is shown in Figure 3, where the along-shore direction reveal velocities peaks of the order of 0.5 m•s-1 in the water column. The near-bottom water current speed in A2 (Figure 2.d) show fluctuations with peaks over 0.1 m•s-1 excepting the mentioned seiche event where peaks arising 0.4 m•s-1.

The near-bottom turbidity shows a fluctuating behavior ranging values from almost zero to higher than 10 NTU (Figure 2.d). In this sense, three differentiated events with high turbidity are observed. These events are E1 (covering from 08:00 of 3rd of August to 10:00 of 5th of August), E2 (03:00 to 12:00 6th of August) and E3 (between 08:00 7th August and 15:00 8th of August). The maximum turbidity is measured during the E1 (maximum turbidity 41.1 NTU). This event lasts for a longer time in comparison to E2 (with a maximum turbidity 4.6 NTU) and E3 (maximum turbidity 12.1 NTU).

3.2 Skill assessment near the sea bottom

The performance of the water circulation model used in this contribution was examined in terms of sea-level, water currents and temperature/salinity evolution in previous works (Cerralbo et al., 2014). However, in this work we pay attention to the near-bottom velocities because its relevant role in the sediment resuspension and transport dynamics. Thus, the skill assessment of the near-bottom velocities in A1 and A2 is analyzed using Taylor diagram (Taylor, 2001). This diagram characterizes the similarity between numerical model and observations using their correlation, the root-mean-square difference (RMSD) and the amplitude of their variations (represented by their standard deviations). The model skill improves as the points get closer to the observation reference point in the diagram (Figure 4). In general, the model results showed a good agreement with the observations in the prevalent along-shelf direction, with correlations larger than 0.5 and RMSD below 1. In addition, the water current fluctuations are well represented in the model because the normalized standard deviation is closer to 1 in both measuring points.

3.3 Modelled bottom stress

The bottom stress is obtained from the coupled numerical model implemented in Alfacs Bay. The Figures 5 and 6 show different snapshots in order to examine the bottom stress pattern for both components (i.e. wave and current-induced bottom stresses). These snapshots corresponds to different episodes identified from the previous observational analysis. The plot scale of the bottom stress is transformed in log10 for clarity. During the case E1 (3rd of August 2013; 10:00 hr) the combined bottom stresses are mainly due to the current bottom stress (Figure 5.left). Maximum values of 0.15 Pa for the combined bottom stress are obtained in the center of the bay and the mouth. This episode corresponds to a seiche event and the spatial variability of the bottom stress is consistent with the spatial pattern of the node/antinode position. It means that the maximum combined bottom stress (associated at maximum water currents) corresponds to the node position (minimum sea-level amplitude). In opposite, the minimum bottom stress corresponds to the antinode position (maximum sea-level amplitude). The position A2 is located near to the node, where the water currents are maximum during the seiche event (0.08 Pa for combined bottom stress). It is worth to mention the node/antinode pattern of the current-induced bottom stress, which presumably would indicate a large spatial variability on the resuspension process within the bay.

After the seiche activity (second stage of E1 where the wind speed increase due to the sea-breeze), the current-induced bottom stress (5th of August 2013; 08:00) decreases significantly in particular in the center of the bay (Figure 5.right). The bottom stress distribution shows how the maximum values are obtained near the shoreline (2.2 Pa) due to the contribution of the wave-induced bottom stress. In A2, the combined bottom stress is equal to 0.03 Pa (value presumably far to induce resuspension). For this event, the wave field during the sea-breeze is shown in Figure 7. This figure shows how the maximum significant wave height (equal to 0.3 m) occurs near the northern and southern shallow edge consistent with the maximum wave-induced bottom stress.

The bottom-stress pattern during the episode E2 (Figure 6.left) is similar to the second stage of the episode E1. Both wave and current bottom stress (08:00 7th of August) tends to be small in A2 in comparison to the seiche event. Only substantial bottom stress are observed in the shallow edges of the bay due to the wave action originated by the sea-breeze.

During the episode E3 (NW wind, Figure 6.right), the combined bottom stress (23:00 8th of August) is dominated by both wave and current action. The southern part of the bay shows the maximum wave induced bottom stress consistent with the wave climate (Figure 7). Also, the current induced bottom stress presents non negligible values within the bay. Focusing in A2, both mechanism contribute in similar manner (wave and current bottom stress is 0.09 and 0.06 Pa respectively) in the combined bottom stress.

4 Discussion

The synchronous time-series of the meteo-oceanographic variables and turbidity shown in Figure 2, jointly with the bottom stress modelled provides a good opportunity to characterize the turbidity peaks measured in A2. During the first stage of the episode E1, the bottom current speed responds at the node-antinode pattern with velocities that raise 0.4 m•s-1 in A2.

Apparently, this increase of the bottom velocity caused bottom sediment resuspension and a turbidity peak (Figure 2). Even that an increase of wind speed occurs (peaks that raise 8 m•s-1), the oscillating pattern of the current (see Figure 3), strongly polarized following the along-shore direction with 1-hr period, suggest an increase of turbidity due to the seiche instead of wind driven current. The bottom stress modeled during E1 (Figure 5) also suggested that the seiche is the main mechanism for turbidity increase in A2 during the first stage of event E1. Resupension mechanism in water environments caused by seiches are suggested in observational investigations (Chung et al., 2009; Jordi et al., 2011; Niedda and Greppi, 2007). However, the numerical results of the current-induced bottom stress shown in Figure 5(left) suggest a high spatial variability of the seiche-induced resuspension not examined in the mentioned contributions. It means observational results about turbidity variability may differ significantly in function of the location of the node/anti-node and its consequent maximum and minimum velocities. The turbidity still shows large values after the seiche was already dissipated and the bottom current decreased during the second stage of the E1 event. Typical sea-breeze wind conditions were observed (gentle variation of wind direction from 30º to 180º) with a noticeable increase of the wind speed during 4th of August unrelated with the current bottom intensity measured. (Llebot et al., 2014) and (Cerralbo et al., 2015a) stated that water current profile due to winds observed in Alfacs Bay does not imply a barotropic shape in the water column, suggesting near the bottom a different behaviour than surface, related to wind set-up phenomena. In consequence, the local resuspension due to wind-breeze seems unlikely at this location of the bay. It seems more feasible that high turbidity measured in A2 during E1 (second stage) are associated to advection of fine sediment resuspended previously by seiche or by sea-breeze activity in the shallow edges of the bay, with a subsequent transport towards the middle of the bay. This last mechanism would explain also the turbidity peak measured during the 5th of August at 00:00; after the fine sediment settling occurred within the bay. The sediment advection within the bay is difficult to confirm according to our data set, but Alfacs bathymetry shows a characteristic shallow edge near the coastline (water depths below 2 m; see Figure 1). In these shallow edges the bottom stress arise 0.8 Pa, suggesting a potential sediment resuspension. This shallow edge may be a source of fine sediment under energetic wind conditions in case of fine sediment availability. In consequence, the advection of resuspended sediment highlight the relevance of the water current patterns within the bay for turbidity measurements.

The episode E2 is associated at sea-breeze mechanism. This event is qualitatively less important in terms of turbidity measured in A2. The comparison of the sea-breeze event during 4th of August and 6th of August (both have similar wind and bottom current speed but different turbidity values) seems to indicate the relevance of the previous events and the subsequent advection of fine sediment following the mechanism way explained previously. Similar to the second stage of E1, in central basin of the bay, the bottom stress are small (below 0.02 Pa); so the local resuspension is unlikely. In consequence, the turbidity measured in A2 is probably due to advection processes of suspended sediment from the shallowest areas (combined bottom stress more than 0.8 Pa) to the central basin.

Finally, episode E3 corresponds to a strong NW wind event with intensities that raise 12 m•s-1. The bottom current speed does not show significant higher values during this episode in comparison to calm periods. However, in opposite to sea breeze, the sea waves generated by the NW wind conditions may have a relevant role in the resuspension mechanisms due to an increase

of the wave induced bottom stress (Figure 6(right)). Unhopefully, the set-up of the ADCP did not allowed to record the oscillatory pattern derived from the orbital velocities generated by waves and the relative importance of each resuspension mechanism (i.e. wind or waves) is difficult to quantify.

E2 and E3 are examples of two mechanisms that may produce local peaks in turbidity: wind-driven current and wind-waves. In Alfacs Bay, the role of these mechanisms in sediment resuspension is less clear in comparison to seiches because they are in function of wind speed without a clear correlation between wind module and the turbidity observed. The resuspension of fine sediment due to wind and wind-waves in shallow environments have been reported in the literature (Bever et al., 2011; Grifoll et al., 2014b; Guillén et al., 2006; Hawley et al., 2014; López et al., 2017; Luettich et al., 1990; Martyanov and Ryabchenko, 2016; Ogston et al., 2000). Some of these works highlight the complexity of the sediment processes due to the temporal and spatial variability of the resuspension mechanisms and the presence of available material to be resuspended. Apparently, this is the case of our observations, because similar wind conditions does not imply the same turbidity measurements. A good example is the sea-breeze wind events during 4th, 5th and 6th of August in which different turbidity values are observed. As we mention in the previous section, advective fluxes and the sequence of events may have a relevant role in the observed water turbidity. In this sense, many authors have reported an evident influence on advective fluxes correlated with suspended sediment concentration after an initial deposition of fine sediment (Bever et al., 2009; Grifoll et al., 2014b; Guillén et al., 2006; Harris et al., 2008; Ogston et al., 2000; Sherwood et al., 1994). This means that on longer time scales, advection of sediment by currents may redistribute sediment and determine final deposition patterns (Wright and Nittrouer, 1995). This may be the mechanism responsible of high turbidity observed under relative low hydrodynamic conditions. For instance, the fact that during the sea-breeze event of 2nd August does not appears high turbidity in opposite to 5th of August (second stage of E1 event) may response at this mechanism where an energetic event (i.e. seiche) may mobilize sediment that after is resuspended easily in subsequent events. The lack of proportionality of the resuspension related to hydrodynamics is also found in extended data time-series where divergences are associated mainly at sediment availability in the bottom among other factors (e.g. in (López et al., 2017; Wiberg et al., 1994)). In the case of Alfacs Bay, more extended observations may clarify the relation between wind intensity, wind-waves, seiches and the amount of suspended sediment and fluxes taking into account the sequence of energetic events.

The sediment distribution in Alfacs Bay (high percentage of silt and clay in the central basin and sand prevalence in the southern, eastern and western shore) is consistent with the modeling results shown in this contribution, where larger bottom stresses were obtained in the lateral shallow edges due to the contribution of the wave induced bottom stress in shallow areas. However, the deposition mechanism may be a complex process including an initial settling and a subsequent dispersal in a similar pattern to described in (Wright and Nittrouer, 1995). Further sediment transport simulations, including sediment classes and erosion and settling effects, would help to investigate the sediment settling dynamics and its final deposition. These processes must take into account the cohesive nature of the fine sediment or others phenomena, such as armoring or bioturbation, that may modify the physical properties of the sediment layers (Amoudry and Souza, 2011; van Ledden et al., 2004).

The bay geometry characteristics (for instance the relative narrow and shallow entrance) suggest the trapping effect of fine sediment delivered by the freshwater outflow or the link between the open sea and the inner bay. The trapping effect of the bay may entailed the presence of a thin surface bottom layer of fine sediment easily involved in resuspension. This behavior is typical from shallow and sheltered environments such as lagoons or lakes. According to (Luettich et al., 1990) and (Hofmann et al., 2011), the regular resuspension events in sheltered and shallow water bodies prevent the sediment consolidation and the formation of a cohesive sediment layer. This may be consistent with the turbidity values observed in the Alfacs Bay under relative weak conditions such as sea-breeze events, as opposite to be expected if the sediment was cohesive.

The image with unprecedent resolution obtained by the Sentinel-2 should allow to identify scenarios with resuspension linked to hydrodynamic forcing. Figure 8 shows the Total Suspended Matter (TSM in mgr•l-1) for the Alfacs Bay in two differentiate scenarios: NW wind and Calm conditions. Without access to local calibration data, a generalized approach for TSM retrieval has been applied. Through SNAP (v. 6.0.0) the Level 1C Sentinel-2 MSI data was converted to geophysical values (suspended sediment concentration) using the most recent version of the water quality processor 'C2RCC' (v. 1.0). The C2RCC processor was run using default values. Following processing in SNAP the data was post-processed (tiles merged and data noise corrected) and the TSM maps created. NW wind conditions increase substantially the TSM in the southeastern shallow edges. This would be a source of a subsequent advection of fine sediment towards the central bay as it was stated in the previous paragraphs. In opposite, the values of TSM decrease significantly during calm conditions.

Also, the proximity of the Ebro river mouth (15 km at north) may increase the suspended sediment within the bay under particular circumstance. River discharge is the main driver of the Ebro River plume, followed by wind and regional oceanic circulation that tends to be southward (Fernández-Nóvoa et al., 2015; Mestres et al., 2003). Analysis of the turbid plume by remote sensing products indicate that more than 70% of the plume extension was located south of the river mouth influenced by the regional oceanic circulation (Fernández-Nóvoa et al., 2015). Others external sediment sources may be associated freshwater discharge from channels, overwash in the bar, flash flood from small creeks or aeolian transport. The complete study of the suspended sediment dynamics will provide objective information to address the problem of degrading water quality within the bay and how to make use of natural mechanisms to limit undesired concentrations of nutrients or pollutants. This applies in particular to harmful algae blooms prone to occur in the area under present and future conditions.

5 Conclusions

The observational set and the wave-current numerical results obtained for Alfacs Bay have permitted to investigate the resuspension mechanisms of fine sediment. The results evidence a clear mechanism of resuspension induced by eventual seiche events, which according to the bottom stress patterns may have a relevant spatial variability within the bay. The wind and wind-wave mechanisms also are responsible of fine sediment resuspension during energetic wind events, especially in shallower areas of the bay. The relevance of the sequence of events in turbidity is highlighted, taking into account the effect of advective sediment fluxes within the bay (from the lateral shallow edges to the middle of the bay). The trapping effect of

the bay may entail the presence of a thin surface layer of fine sediment easily involved in resuspension neglecting the expected cohesive effects. However, these points deserve further analysis with extended data sets and sediment transport modeling. The exchange of fine sediment within the bay and the open sea seems also evident according to remote sensing images. However, these points deserve further analysis with extended data sets and sediment transport modeling. As a region of high-anthropogenic pressure, this research may contribute to develop better integrated plans in the context of sustainable aquaculture activities and the mitigation of the effects of climate change in the Ebro Delta.

Acknowledgments

The authors are grateful for the collaboration IRTA staff for the participation in the field campaigns carried out within the framework of the monitoring program of water quality at the shellfish growing areas in Catalonia. Thanks to the data provided by Puertos del Estado and AEMET. This work received funding from the EU H2020 program under grant agreement no. 730030 (CEASELESS project). We also want to thank to Secretaria d'Universitats i Recerca del Dpt. d'Economia i Coneixement de la Generalitat de Catalunya (Ref 2014SGR1253) who support our research group. The paper contains modified Copernicus Sentinel data [2017/2018].

References

Amoudry, L. O. and Souza, A. J.: Deterministic coastal morphological and sediment transport modeling: a review and discussion, Rev. Geophys., (49), 1–21, doi:10.1029/2010RG000341.1.INTRODUCTION, 2011.

Bever, A. J., Harris, C. K., Sherwood, C. R. and Signell, R. P.: Deposition and flux of sediment from the Po River, Italy: An idealized and wintertime numerical modeling study, Mar. Geol., 260(1–4), 69–80, doi:10.1016/j.margeo.2009.01.007, 2009.

Bever, A. J., McNinch, J. E. and Harris, C. K.: Hydrodynamics and sediment-transport in the nearshore of Poverty Bay, New Zealand: Observations of nearshore sediment segregation and oceanic storms, Cont. Shelf Res., 31(6), 507–526, doi:10.1016/j.csr.2010.12.007, 2011.

Booij, N., Ris, R. C. and Holthuijsen, L. H.: A third-generation wave model for coastal regions: 1. Model description and validation, J. Geophys. Res., 104(C4), 7649, doi:10.1029/98JC02622, 1999.

Camp, J. and Delgado, M.: Hidrografía de las bahías del delta del Ebro, Investig. Pesq., 51(3), 351–369, 1987.

Carlin, J. A., Lee, G. hong, Dellapenna, T. M. and Laverty, P.: Sediment resuspension by wind, waves, and currents during meteorological frontal passages in a micro-tidal lagoon, Estuar. Coast. Shelf Sci., 172, 24–33, doi:10.1016/j.ecss.2016.01.029, 2016.

Cerralbo, P., Grifoll, M., Valle-Levinson, A. and Espino, M.: Tidal transformation and resonance in a short, microtidal Mediterranean estuary (Alfacs Bay in Ebre delta), Estuar. Coast. Shelf Sci., 145, doi:10.1016/j.ecss.2014.04.020, 2014.

Cerralbo, P., Grifoll, M. and Espino, M.: Hydrodynamic response in a microtidal and shallow bay under energetic wind and

seiche episodes, J. Mar. Syst., 149, doi:10.1016/j.jmarsys.2015.04.003, 2015a.

Cerralbo, P., Grifoll, M., Moré, J., Bravo, M., Sairouní Afif, a. and Espino, M.: Wind variability in a coastal area (Alfacs Bay, Ebro River delta), Adv. Sci. Res., 12, 11–21, doi:10.5194/asr-12-11-2015, 2015b.

Cerralbo, P., Espino, M. and Grifoll, M.: Modeling circulation patterns induced by spatial cross-shore wind variability in a small-size coastal embayment, Ocean Model., 104, doi:10.1016/j.ocemod.2016.05.011, 2016.

Cerralbo, P., Espino, M., Grifoll, M., and Valle-Levinsion, A: Subtidal circulation in a microtidal Mediterranean bay, Sci. Mar. 82(4): 231-243, doi:10.3989/scimar.4801.16A, 2018.

Chung, E. G., Bombardelli, F. A. and Schladow, S. G.: Sediment resuspension in a shallow lake, Water Resour. Res., 45(5), 1–18, doi:10.1029/2007WR006585, 2009.

Ellis, J., Cummings, V., Hewitt, J., Thrush, S. and Norkko, A.: Determining effects of suspended sediment on condition of a suspension feeding bivalve (Atrina zelandica): Results of a survey, a laboratory experiment and a field transplant experiment, J. Exp. Mar. Bio. Ecol., 267(2), 147–174, doi:10.1016/S0022-0981(01)00355-0, 2002.

Fan, S., Swift, D. J. P., Traykovski, P., Bentley, S., Borgeld, J. C., Reed, C. W. and Niedoroda, A. W.: River flooding, storm resuspension, and event stratigraphy on the northern California shelf: observations compared with simulations, Mar. Geol., 210(1–4), 17–41, doi:10.1016/j.margeo.2004.05.024, 2004.

Fernández-Nóvoa, D., Mendes, R., deCastro, M., Dias, J. M., Sánchez-Arcilla, A. and Gómez-Gesteira, M.: Analysis of the influence of river discharge and wind on the Ebro turbid plume using MODIS-Aqua and MODIS-Terra data, J. Mar. Syst., 142, 40–46, doi:10.1016/j.jmarsys.2014.09.009, 2015.

Garel, E., Pinto, L., Santos, A. and Ferreira, Ó.: Tidal and river discharge forcing upon water and sediment circulation at a rock-bound estuary (Guadiana estuary, Portugal), Estuar. Coast. Shelf Sci., 84(2), 269–281, doi:10.1016/j.ecss.2009.07.002, 2009.

Ghosh, L. K., Prasad, N., Joshi, V. B. and Kunte, S. S.: A study on siltation in access channel to a port, Coast. Eng., 43(1), 59–74, doi:10.1016/S0378-3839(01)00006-0, 2001.

Giannakourou, A., Orlova, T. Y., Assimakopoulou, G. and Pagou, K.: Dinoflagellate cysts in recent marine sediments from Thermaikos Gulf, Greece: Effects of resuspension events on vertical cyst distribution, Cont. Shelf Res., 25(19–20), 2585–2596, doi:10.1016/j.csr.2005.08.003, 2005.

Grifoll, M., Gracia, V., Fernandez, J. and Espino, M.: Suspended sediment observations in the Barcelona inner-shelf during storms, J. Coast. Res., (SPEC. ISSUE 65), doi:10.2112/SI65-259, 2013.

Grifoll, M., Gracia, V., Aretxabaleta, A. L., Guillén, J., Espino, M. and Warner, J. C.: Formation of fine sediment deposit from a flash flood river in the Mediterranean Sea, J. Geophys. Res. Ocean., 119, 5837–5853, doi:10.1002/2014JC010187, 2014a.

Grifoll, M., Gracia, V., Aretxabaleta, A., Guillén, J., Espino, M. and Warner, J. C.: Formation of fine sediment deposit from a flash flood river in the Mediterranean Sea, J. Geophys. Res. C Ocean., 119(9), doi:10.1002/2014JC010187, 2014b.

Grifoll, M., Aretxabaleta, A. L. and Espino, M.: Shelf response to intense offshore wind, J. Geophys. Res. C Ocean., 120(9), 6564–6580, doi:10.1002/2015JC010850, 2015.

Grifoll, M., Navarro, J., Pallares, E., Ràfols, L., Espino, M. and Palomares, A.: Ocean–atmosphere–wave characterisation of a wind jet (Ebro shelf, NW Mediterranean Sea), Nonlinear Process. Geophys., 23(3), 143–158, doi:10.5194/npg-23-143-2016, 2016.

Guillen, J. and Palanques, A.: A shoreface zonation in the Ebro Delta based on grain size distribution, J. Coast. Res., 13(3), 867–878 [online] Available from: http://www.scopus.com/inward/record.url?eid=2-s2.0-0030746817&partnerID=tZOtx3y1, 1997.

Guillén, J., Palanques, a, Puig, P. and Durrieu de Madron, X.: Field calibration of optical sensors for measuring suspended sediment concentration in the western Mediterranean, Sci. Mar., 64(4), 427–435, doi:10.3989/scimar.2000.64n4427, 2000.

Guillén, J., Bourrin, F., Palanques, a., Durrieu de Madron, X., Puig, P. and Buscail, R.: Sediment dynamics during wet and dry storm events on the Têt inner shelf (SW Gulf of Lions), Mar. Geol., 234(1–4), 129–142, doi:10.1016/j.margeo.2006.09.018, 2006.

Harris, C. K., Sherwood, C. R., Signell, R. P., Bever, A. J. and Warner, J. C.: Sediment dispersal in the northwestern Adriatic Sea, J. Geophys. Res., 113(C11), C11S03, doi:10.1029/2006JC003868, 2008.

Hawley, N., Redder, T., Beletsky, R., Verhamme, E., Beletsky, D. and DePinto, J. V.: Sediment resuspension in Saginaw Bay, J. Great Lakes Res., 40(S1), 18–27, doi:10.1016/j.jglr.2013.11.010, 2014.

Hofmann, H., Lorke, A. and Peeters, F.: Wind and ship wave-induced resuspension in the littoral zone of a large lake, Water Resour. Res., 47(9), 1–12, doi:10.1029/2010WR010012, 2011.

Jacob, R., Larson, J. and and Ong, E.: {M}\cdotn communication and parallel interpolation in {CCSM3} using the {M}odel {C}oupling {T}oolkit, Int. J. High Perf. Comp. App., 19, 293–308, 2005.

Jordi, A., Basterretxea, G., Casas, B., Anglès, S. and Garcés, E.: Seiche-forced resuspension events in a Mediterranean harbour, Cont. Shelf Res., 28(4–5), 505–515, doi:10.1016/j.csr.2007.10.009, 2008.

Jordi, A., Basterretxea, G. and Wang, D.-P.: Local versus remote wind effects on the coastal circulation of a microtidal bay in the Mediterranean Sea, J. Mar. Syst., 88(2), 312–322 [online] Available from: http://www.sciencedirect.com/science/article/pii/S0924796311001266, 2011.

Kumar, N., Voulgaris, G., Warner, J. C. and Olabarrieta, M.: Implementation of the vortex force formalism in the coupled ocean-atmosphere-wave-sediment transport (COAWST) modeling system for inner shelf and surf zone applications, Ocean Model., 47, 65–95, doi:10.1016/j.ocemod.2012.01.003, 2012.

van Ledden, M., van Kesteren, W. G. . and Winterwerp, J. .: A conceptual framework for the erosion behaviour of sand–mud mixtures, Cont. Shelf Res., 24(1), 1–11, doi:10.1016/j.csr.2003.09.002, 2004.

Llebot, C., Spitz, Y. H., Sol??, J. and Estrada, M.: The role of inorganic nutrients and dissolved organic phosphorus in the phytoplankton dynamics of a Mediterranean bay: A modeling study, J. Mar. Syst., 83(3–4), 192–209, doi:10.1016/j.jmarsys.2010.06.009, 2010.

Llebot, C., Solé, J., Delgado, M., Fernández-Tejedor, M., Camp, J. and Estrada, M.: Hydrographical forcing and phytoplankton variability in two semi-enclosed estuarine bays, J. Mar. Syst., 86(3–4), 69–86, doi:10.1016/j.jmarsys.2011.01.004, 2011.

Llebot, C., Rueda, F. J., Solé, J., Artigas, M. L. and Estrada, M.: Hydrodynamic states in a wind-driven microtidal estuary (Alfacs Bay), J. Sea Res., 85, 263–276, doi:10.1016/j.seares.2013.05.010, 2014.

López, L., Guillén, J., Palanques, A. and Grifoll, M.: Seasonal sediment dynamics on the Barcelona inner shelf (NW Mediterranean): A small Mediterranean river- and wave-dominated system, Cont. Shelf Res., 145, doi:10.1016/j.csr.2017.07.008, 2017.

Loureiro, S., Garcés, E., Fernández-Tejedor, M., Vaqué, D. and Camp, J.: Pseudo-nitzschia spp. (Bacillariophyceae) and dissolved organic matter (DOM) dynamics in the Ebro Delta (Alfacs Bay, NW Mediterranean Sea), Estuar. Coast. Shelf Sci., 83(4), 539–549, doi:10.1016/j.ecss.2009.04.029, 2009.

Luettich, R. A. J., Harleman, D. R. F. and Somlyódy, L.: Dynamic behavior of suspended sediment concentrations in a shallow lake perturbed by episodic wind events, Limnol. Oceanogr., 35(5), 1050–1067, doi:10.4319/lo.1990.35.5.1050, 1990.

van Maren, D. S., van Kessel, T., Cronin, K. and Sittoni, L.: The impact of channel deepening and dredging on estuarine sediment concentration, Cont. Shelf Res., 95, 1–14, doi:10.1016/j.csr.2014.12.010, 2015.

Martyanov, S. and Ryabchenko, V.: Bottom sediment resuspension in the easternmost Gulf of Finland in the Baltic Sea: A case study based on three-dimensional modeling, Cont. Shelf Res., 117, 126–137, doi:10.1016/j.csr.2016.02.011, 2016.

Mehta, A. J.: On estuarine cohesive sediment suspension behavior, J. Geophys. Res. Ocean., 94(C10), 14303–14314, doi:10.1029/JC094iC10p14303, 1989.

Mestres, M., Sierra, J. P. A. U., Sánchez-Arcilla, A., González, J., Río, D. E. L., Wolf, T. and Rodríguez, A.: Modelling of the Ebro River plume . Validation with field observations, Scientia Marina, 67(4), 379–391, 2003.

Newcombe, C. P. and Macdonald, D. D.: Effects of Suspended Sediments on Aquatic Ecosystems, North Am. J. Fish. Manag., 11(1), 72–82, doi:10.1577/1548-8675(1991)011<0072:EOSSOA>2.3.CO;2, 1991.

Niedda, M. and Greppi, M.: Tidal, seiche and wind dynamics in a small lagoon in the Mediterranean Sea, Estuar. Coast. Shelf Sci., 74(1–2), 21–30, doi:10.1016/j.ecss.2007.03.022, 2007.

Ogston, A. ., Cacchione, D. ., Sternberg, R. . and Kineke, G. .: Observations of storm and river flood-driven sediment transport on the northern California continental shelf, Cont. Shelf Res., 20(16), 2141–2162, doi:10.1016/S0278-4343(00)00065-0, 2000.

Palacín, C., Martin, D. and and Gili, J. M.: Features of spatial distribution of benthic infauna in a Mediterranean shallow-water Bay, Mar. Biol., 321, 315–321, 1991.

Palanques, A., Lopez, L., Guillén, J., Puig, P. and Masqué, P.: Decline of trace metal pollution in the bottom sediments of the Barcelona City continental shelf (NW Mediterranean), Sci. Total Environ., 579, 755–767, doi:10.1016/j.scitotenv.2016.11.031, 2017.

Ramírez-Pérez, M., Gonçalves-Araujo, R., Wiegmann, S., Torrecilla, E., Bardaji, R., Röttgers, R., Bracher, A. and Piera, J.: Towards cost-effective operational monitoring systems for complex waters: Analyzing small-scale coastal processes with optical transmissometry, PLoS One, 12(1), 1–21, doi:10.1371/journal.pone.0170706, 2017.

Roque, A., Lopez-Joven, C., Lacuesta, B., Elandaloussi, L., Wagley, S., Furones, M. D., Ruiz-Zarzuela, I., De Blas, I., Rangdale, R. and Gomez-Gil, B.: Detection and identification of tdh- And trh-positive Vibrio parahaemolyticus strains from

four species of cultured bivalve molluscs on the Spanish Mediterranean coast, Appl. Environ. Microbiol., 75(23), 7574–7577, doi:10.1128/AEM.00772-09, 2009.

Satta, C. T., Anglès, S., Lugliè, A., Guillén, J., Sechi, N., Camp, J. and Garcés, E.: Studies on dinoflagellate cyst assemblages in two estuarine Mediterranean bays: A useful tool for the discovery and mapping of harmful algal species, Harmful Algae, 24, 65–79, doi:10.1016/j.hal.2013.01.007, 2013.

Shchepetkin, A. F. and McWilliams, J. C.: The regional oceanic modeling system (ROMS): a split-explicit, free-surface, topography-following-coordinate oceanic model, Ocean Model., 9(4), 347–404, doi:10.1016/j.ocemod.2004.08.002, 2005.

Sherwood, C. R., Butman, B., Cacchione, D. A., Drake, D. E., Gross, T. F., Sternberg, R. W., Wiberg, P. L. and Williams, A. J.: Sediment-transport events on the northern California continental shelf during the 1990–1991 STRESS experiment, Cont. Shelf Res., 14(10–11), 1063–1099, doi:10.1016/0278-4343(94)90029-9, 1994.

Shteinman, B., Eckert, W., Kaganowsky, S. and Zohary, T.: Seiche-Induced Resuspension in Lake Kinneret: A Fluorescent Tracer Experiment, in The Interactions Between Sediments and Water: Proceedings of the 7th International Symposium, Baveno, Italy 22--25 September 1996, edited by R. D. Evans, J. Wisniewski, and J. R. Wisniewski, pp. 123–131, Springer Netherlands, Dordrecht., 1997.

Solé, J., Turiel, A., Estrada, M., Llebot, C., Blasco, D., Camp, J., Delgado, M., Fernández-Tejedor, M. and Diogène, J.: Climatic forcing on hydrography of a Mediterranean bay (Alfacs Bay), Cont. Shelf Res., 29(15), 1786–1800, doi:10.1016/j.csr.2009.04.012, 2009.

Sondergaard, M., Kristensen, P. and Jeppesen, E.: Phosphorus release from ressuspended sediment in the shallow and wind-exposed Lake Arreso, Denmark, Hydrobiologia, 228, 91–99, 1992.

Soulsby, R.: Dynamics of marine sands, Thomas Telford Publishing., 1997.

Styles, R. and Glenn, S. M.: Modeling stratified wave and current bottom boundary layers on the continental shelf, J. Geophys. Res., 105(C10), 24119–24139, doi:10.1029/2000JC900115, 2000.

Taylor, K. E.: Summarizing multiple aspects of model performance in a single diagram, J. Geophys. Res., 106(D7), 7183–7192, doi:10.1029/2000JD900719, 2001.

Warner, J. C., Sherwood, C. R., Signell, R. P., Harris, C. K. and Arango, H. G.: Development of a three-dimensional, regional, coupled wave, current, and sediment-transport model, Comput. Geosci., 34(10), 1284–1306, doi:10.1016/j.cageo.2008.02.012, 2008.

Warner, J. C., Armstrong, B., He, R. and Zambon, J. B.: Development of a Coupled Ocean–Atmosphere–Wave–Sediment Transport (COAWST) Modeling System, Ocean Model., 35(3), 230–244, doi:10.1016/j.ocemod.2010.07.010, 2010.

Wiberg, P. L., Drake, D. E. and Cacchione, D. A.: Sediment resuspension and bed armoring during high bottom stress events on the northern California inner continental shelf: measurements and predictions, Cont. Shelf Res., 14(10), 1191–1219, doi:http://dx.doi.org/10.1016/0278-4343(94)90034-5, 1994.

Wright, L. D. and Nittrouer, C. a.: Dispersal of River Sediments in Coastal Seas: Six Contrasting Cases, Estuaries, 18(3), 494, doi:10.2307/1352367, 1995.

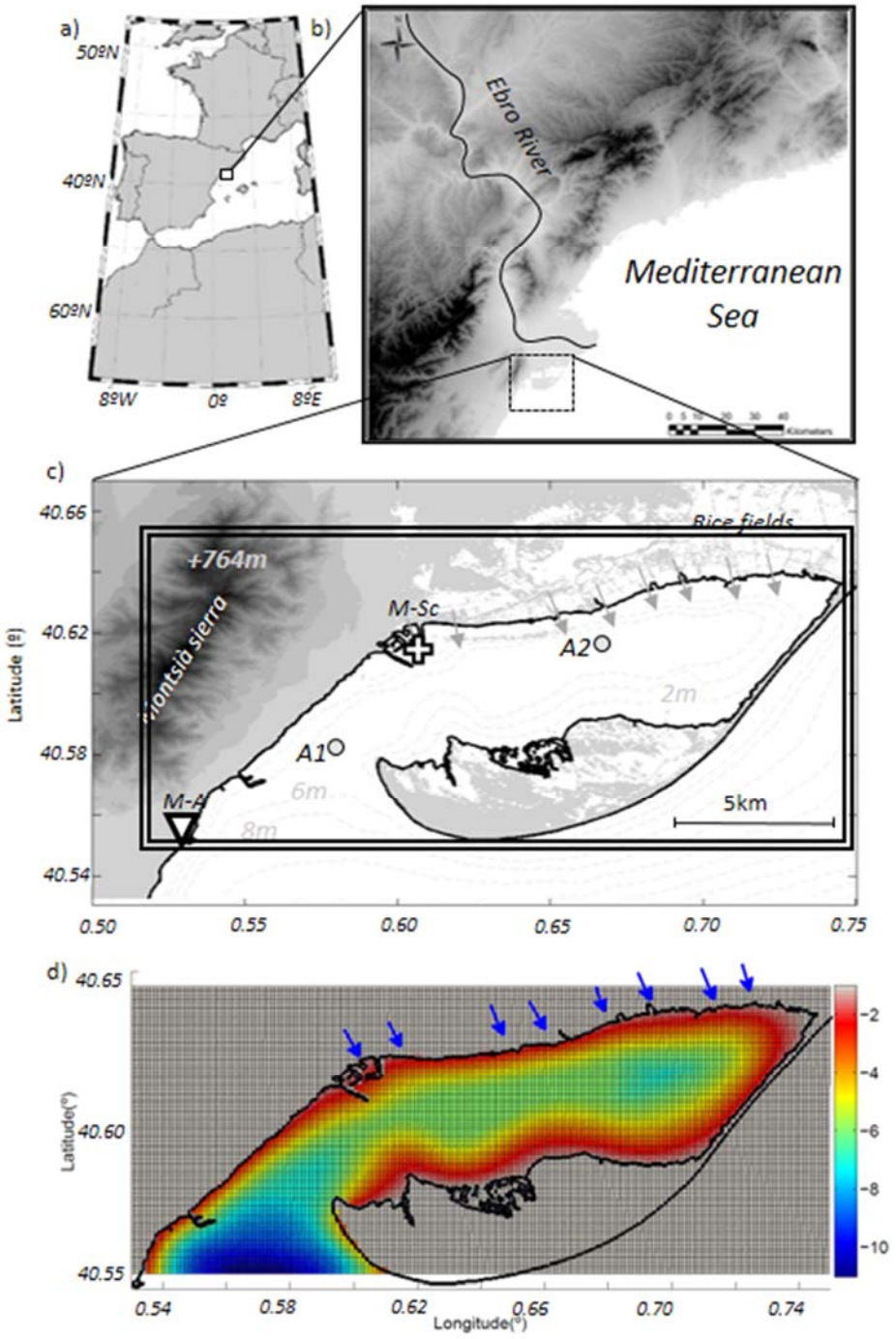

Figure 1: a: Regional location of Ebro River Delta b: Alfacs Bay in Ebro River Delta. c: map of Alfacs Bay. Triangle shows the meteorological station (M-Sc). White cross for Sant Carles de la Ràpita tide gauge. Gray circles shows the ADCP and OBS mooring locations (A1 and A2). Gray arrows on the northern coast shows the freshwater drainage points considered in the simulation. Double line square indicate the domain for the hydrodynamic numerical model, which is shown in detail in

image d (colorbar indicates depth in meters). The background grid corresponds to the numerical mesh used in the numerical modelling. Blue arrows on the northern coast shows the freshwater drainage points considered in the simulation.

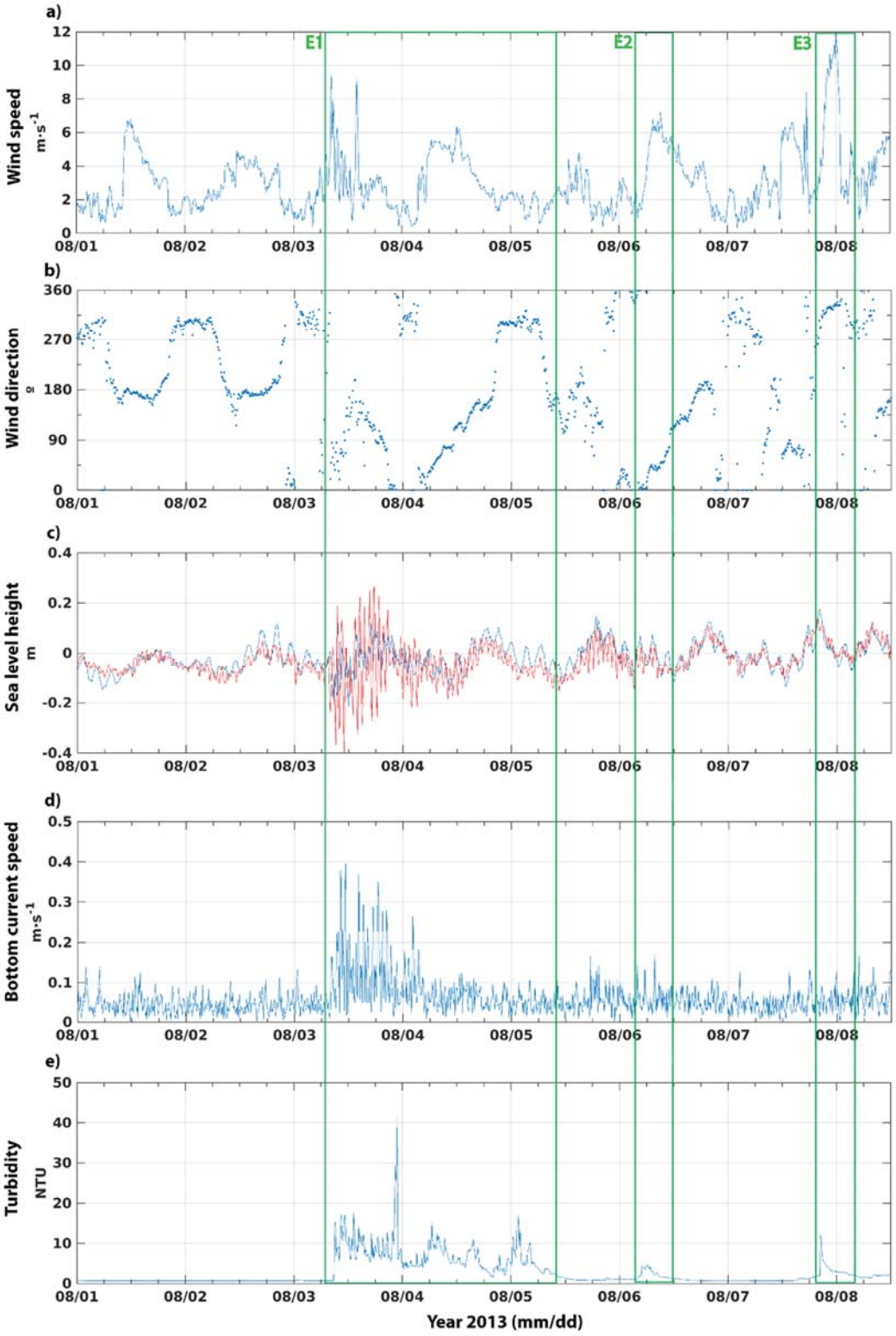
a)
Wind speed
m·s-1
E1
E2
E3
b)
Wind direction
°
c)
Sea level height
m
d)
Bottom current speed
m·s-1
e)
Turbidity
NTU
08/01
08/02
08/03
08/04
08/05
08/06
08/07
08/08
Year 2013 (mm/dd)

495

Figure 2: Time-series of the variables measured during the field campaign. (a) wind intensity measured in M-Sc. (b) wind direction measured in M-Sc. (c) Sea-level height measured in A2 (blue) and A1 (red). (d) near-bottom current velocity measured in A1. (e) NTU measured in OBS mounted at A2 station. Vertical bars show the episodes considered in the analysis.

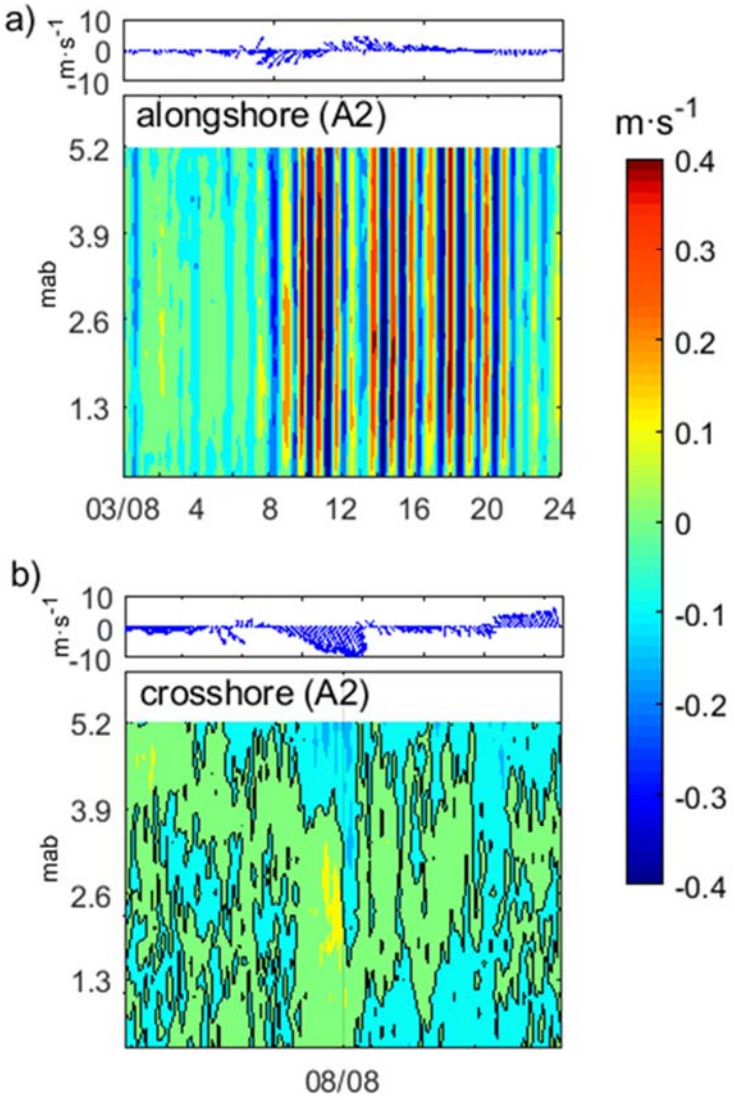

500 **Figure 3: Each panel shows on the top the wind measured at M-Sc (in m·s^{-1}), and on the bottom the vertical profiles velocities measured at A2 (in m·s^{-1}; mab mean meters above the bottom). In each panel, different events are showed: 2013/8/3 for alongshore velocities (panel a) and 2013/8/8 for crosshore (panel b). Black lines show 0 velocity isolines.**

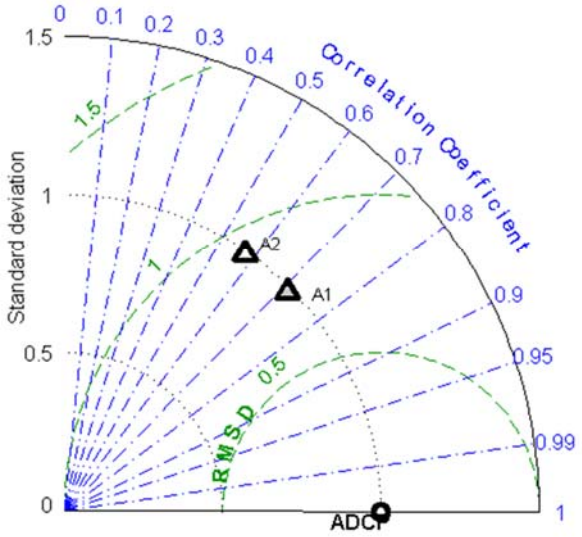

Figure 4: Taylor diagram comparing the error metrics between the observations and model results for the near-bottom currents. A1 and A2 corresponds to the ADCP locations shown in Figure 1.

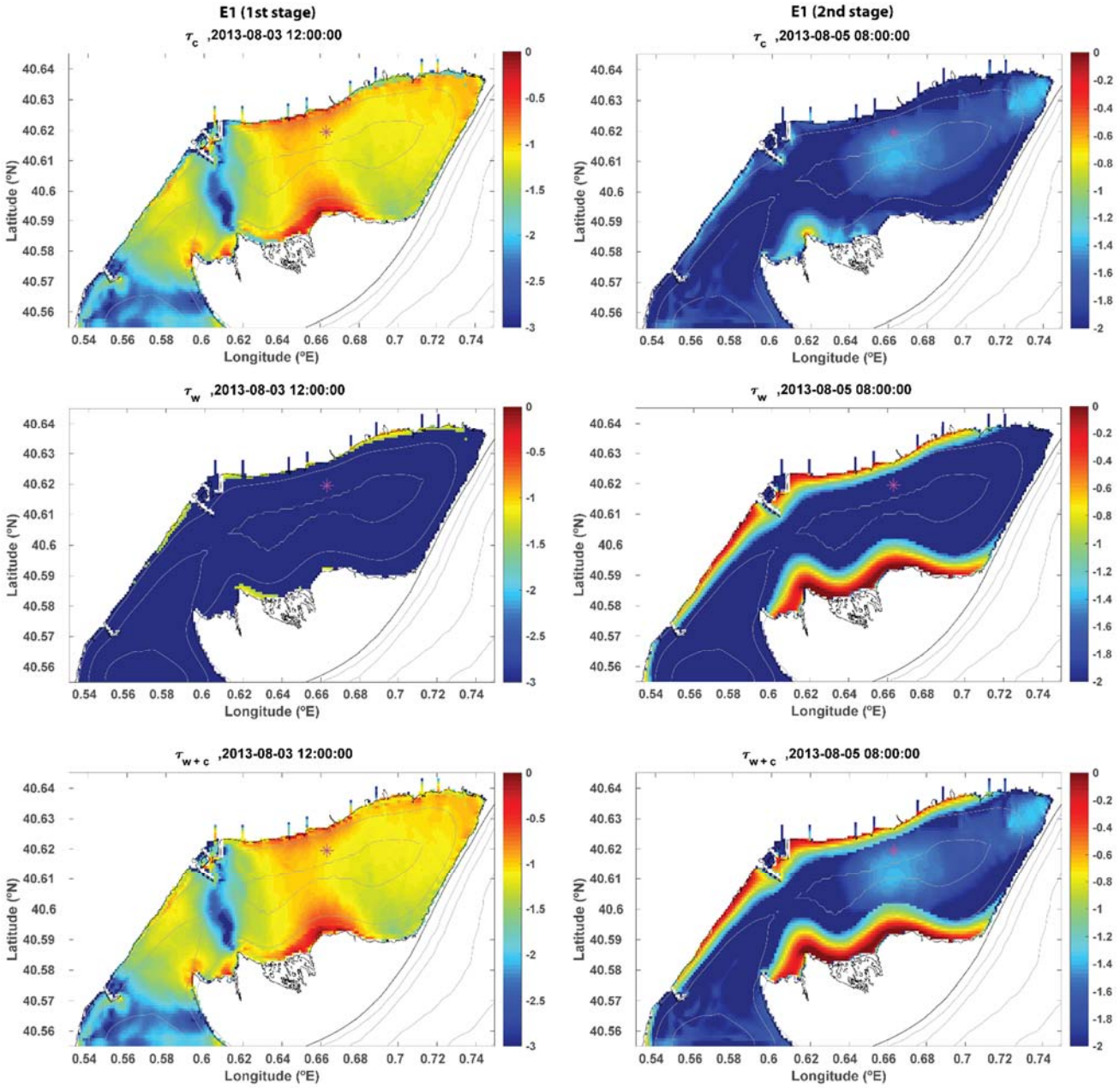

Figure 5: Distribution of the current, wave and combined wave-current bottom stresses log10(Pa) in the Alfacs Bay during the first stage of the episode E1 (i.e. seiche; left panel) and the second stage of the episode E1 (i.e. sea breeze; right panel). Magenta symbol show the A2 station. Isobaths (in grey) are plotted each 3 m. Note that for clarity, the plot scale is transformed in log10 and the vertical range differs between both bottom stress distributions.

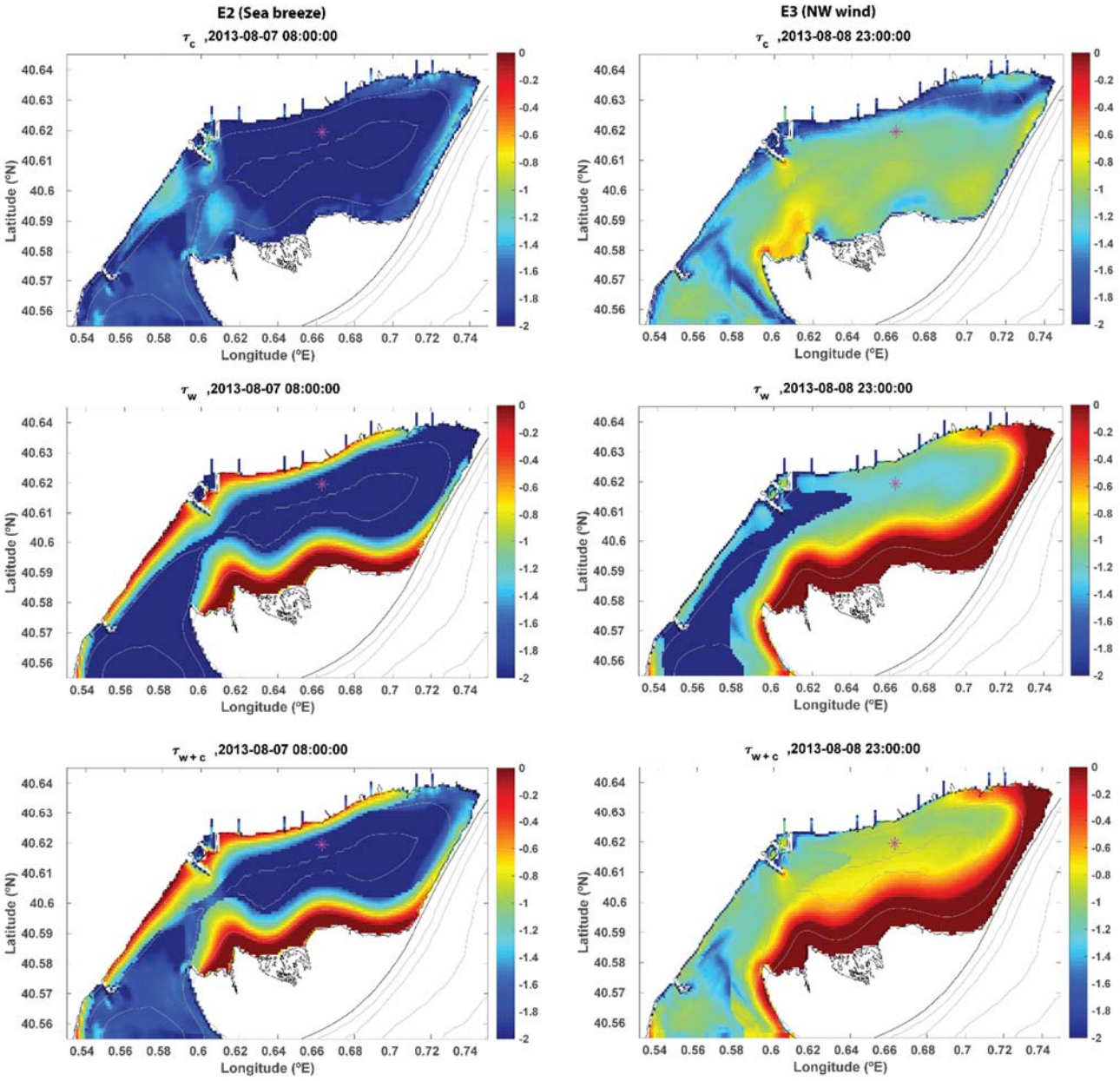

Figure 6: Distribution of the current, wave and combined wave-current bottom stresses log10(Pa) in the Alfacs Bay during the first stage of the episode E2(left) and E3(right). Magenta symbol show the A2 station. Isobaths (in grey) are plotted each 3 m. Note that for clarity, the plot scale is transformed in log10 and the vertical range differs between both bottom stress distributions.

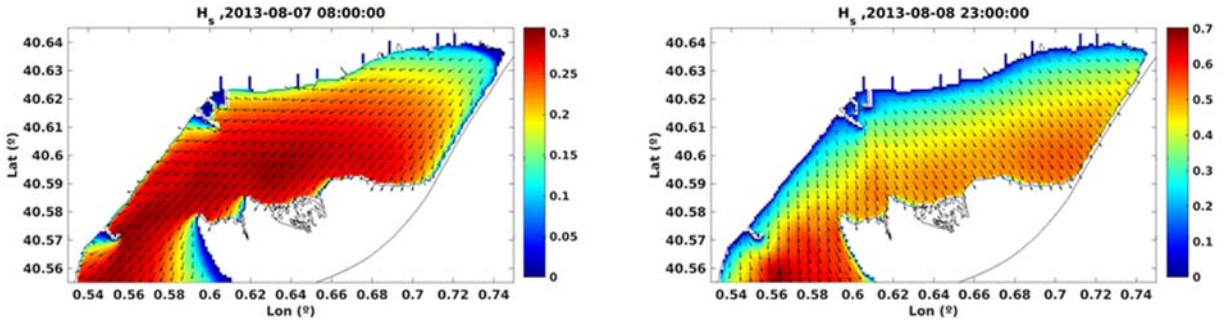

Figure 7: Snapshot of the wave field for the episode E2 (sea-breeze; left) and E3 (NW wind; right). Color map represents the significant wave height and black arrows the direction of propagation. Note that the ranges of the significant wave height are different.

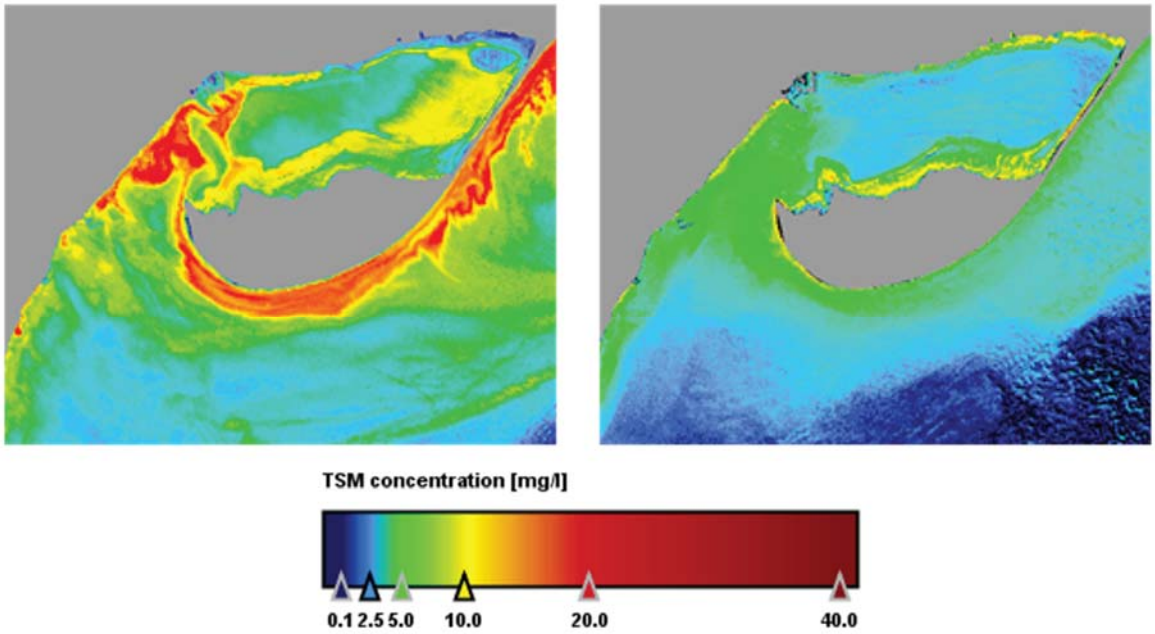

Figure 8: Total Suspended Matter (TSM in mgr•l-1) obtained from Sentinel-2 for the Alfacs Bay in two differentiate scenarios: NW winds (left; 27th of December 2017) and calm conditions (right; 15th of February of 2018).